SAND--89-0101C

DE90 000793

A Pulsed-Power Upgrade Study of PBFA II Based on a Closed Disk Transmission System

L. X Schneider, W. A. Johnson, E. L. Neau, and S. R. Babcock
Sandia National Laboratories
Albuquerque, NM 87185

Abstract

A coax-to-disk transition and disk transformer system has been designed as a possible replacement for the coax-to-flat plate transformer and cross-over system of the Particle Beam Fusion Accelerator II (PBFA II). Together with a simplification of the coaxial pulse-forming lines (PFL's), this predominately closed geometry system increases the energy available for ICF experiments by greater than 50%. Analytical techniques have been combined with single-module scale model experiments and TEM circuit simulations to develop a design that maximizes the energy transport efficiency through the new transmission-line system. Multi-module scale model experiments and 2-D time-dependent electromagnetic simulations have verified these techniques can accurately project the energy transfer efficiency and thereby be used to predict full-scale performance.

Introduction

The existing PFL system of PBFA II [1] delivers energy to an inductive store comprised of vacuum insulated transmission lines located inside of a vacuum insulator stack. Energy is transferred to a dynamic ion beam diode by a Plasma Opening Switch (POS). An energy upgrade study has been completed which defines a design that will increase the energy output of the PFL system as well as improve the transport efficiency of this energy to the inductive store. Data on long pulse POS conduction [2] has demonstrated conduction times to 100 ns, which allows the removal of a stage of pulse compression to increase the energy output of the PBFA II PFL system. Improved energy transport from the modified PFL's to the vacuum stack has been accomplished through the use of an abrupt coax-to-disk transition and disk transformer system which was suggested by an analysis of the dominant losses in the present PBFA II flat-plate transmission system [3]. The upgrade design increases the forward-going energy at the vacuum stack interface from the existing 2.9 MJ to greater than 4.4 MJ while improving the coupling efficiency of this energy to the vacuum inductance. With the PFL modification, total stored energy in the stack will improve from the existing 2.0 MJ to greater than 3.0 MJ.

Pulse-Forming Line Modifications

Figure 1 shows a comparison of the present PBFA II PFL's and the flat-plate transformer system with the upgrade PFL's and closed disk transformer system. Conversion of the present 2.2 ohm PFL's to 3.9 ohms PFL's and removal of a stage of pulse compression increases the energy available in this section of the accelerator from approximately 6.1 MJ to 7.2 MJ, or approximately 200 kJ per module. This modification increases the output pulse width from 40 ns to 95 ns FWHM. The increase in pulse width requires an electrically longer transformer section for efficient operation and therefore reduces the physical space available for the coax-to-disk transition. This disadvantage is offset by the fact that the 3.9 ohm PFL output impedance will require less impedance transformation to couple energy efficiently into the vacuum stack. The longer pulsewidth also reduces the electrical stress on both the vacuum and water side of the insulator, due to the slower risetime pulse, thus allowing increased energy flow through the vacuum insulator without exceeding original design limits.

Testing of the modified PFL components has been completed in DEMON, a PBFA II component test facility, and has demonstrated a TEM output energy of 200 kJ per module in the coax. Waveforms were obtained at four points around the circumference of the output coaxial line and averaged to obtain the TEM forward-going energy by removing possible higher order modes excited by non-uniform water switch closure.

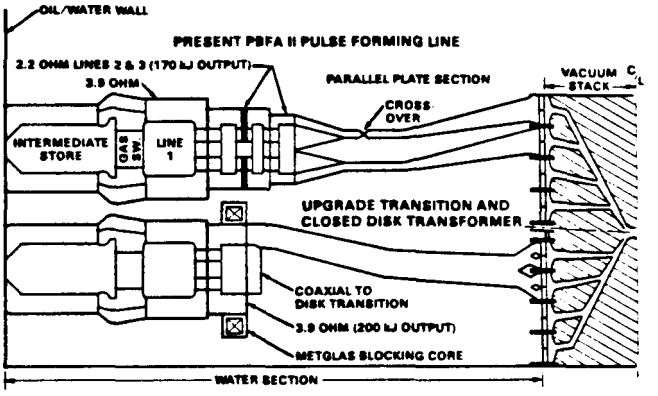

Figure 1. Comparison of the existing Pulse-Forming System of PBFA II (top) and the proposed upgrade design (bottom).

PFL to Vacuum Stack Energy Transport

In the upgrade design, four closed disk transformers confine the energy flow from the existing four layers of nine parallel PFL's to the vertical adder in the vacuum stack. The transformer length requirement and spacial constraints in the existing PFL system led to the design of a compact coax-to-disk transition. Since the efficiency of the transformer is determined solely by the available length for that device, the transition becomes the single source of controllable energy losses in the upgrade design.

Transition Physics

Two significant loss mechanisms are present in the coax-to-disk transition. In the first loss mechanism, energy can couple into the external impedances at the open junction [4]. For the multi-layer geometry of PBFA II, an estimate of junction losses is obtained by an equivalent TEM analysis that considers all closed transmission lines and external impedances. Since the top two and bottom two layers of PBFA II are in parallel, we approximate a mirror symmetry plane between the layers to reduce the analysis of the TEM junction losses to the transmission line system shown in Fig. 2. This 3-D geometry can be represented by a multi-module TEM equivalent circuit model, as shown in Fig. 3, with the assumption of vertical symmetry planes, or magnetic boundaries, which extend radially between the coaxes on a given layer. The impedances shown are on a per module basis and were calculated through the use of a static capacitance solver to determine the capacitance matrix at the transition junction.

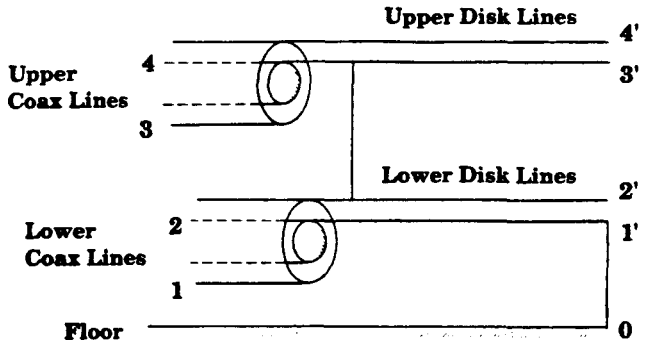

Figure 2. Multi-module transmission system present at the open junction of the coax-to-disk transitions.

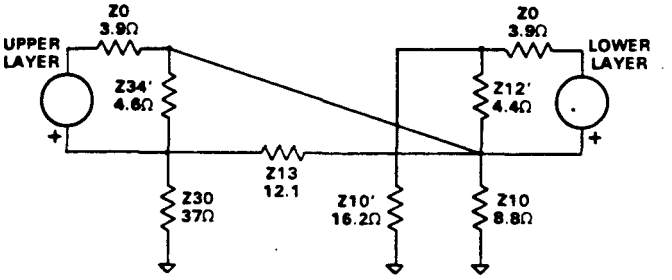

Figure 3. TEM equivalent circuit of the multi-module transmission line system of Fig. 2. Element numbers correspond to the conductors in Fig. 2.

In the circuit model for the lower line, the lower disk impedance, Z12', is in parallel with the external shunt impedance, Z10', and a parallel combination dominated by Z10 in parallel with Z13+Z30. The upper disk impedance, Z34', is shunted by the parallel combination of Z13 and Z30+Z10. To maximize the energy transfer efficiency through these junctions, it is desirable to increase the shunt impedances as high as possible. The most effective means to increase these impedances in PBFA II is to use magnetic blocking cores around the outer coaxial cylinder directly before the transition (See Fig. 1). The effect of the blocking cores on the TEM efficiency of each layer will be discussed later.

The second loss mechanism is more difficult to analyze and control. Each disk transformer is fed by nine coaxial lines; therefore, each coax feeds an equivalent disk segment one-ninth the circumference of the disk transformer. The disk width, at the outer radius, is a large fraction of the wavelength for an appreciable portion of the pulse. Transit time effects through the transition excite higher-order-modes in the disk transformer and back into the PFL and external impedances of the junction. Because the disk transformer represents the lowest impedance to the TEM mode, the majority of the energy loss in the higher-order-modes is in the disk, with cutoff frequencies which are a function only of the disk segment width. These TE modes, which can represent substantial losses, travel slower than the TEM wave and cannot couple efficiently into the vacuum adder. The $TE_{0,m}$ mode can be readily derived for the disk geometry with the assumption of mirror symmetry planes between the coaxes as shown in Fig. 4. Previous work has neglected the radial variation of the disk segment [5]. The electric field variation across the input to the disk segment can be described as,

$$E_z = -j\omega\mu\ \psi_{o,m} \qquad (1)$$

where ω is the frequency in rad/sec, μ the permeability in henrys/m and m the mode number. $\psi_{o,m}$ can be expressed in terms of the Hankel function of the first kind of order 9m/2, and describes the voltage variation across the segment width as,

$$\psi_{o,m} = H^{(1)}_{9m/2}\ (k\rho)\ \cos\left[\frac{9m}{2}\ \phi\right] \qquad (2)$$

where ϕ represents the location across the segment and k is the wave number in water. Since the source and geometry is even about $\phi_o/2$, E_z must be even about $\phi_o/2$ to maintain symmetry and allows the excitation of only even mode numbers. The m=0 mode is TEM to the direction of propagation into the disk. Since the wave impedance is mostly resistive for $k\rho > 9m/2$ and mostly reactive for $k\rho < 9m/2$, a radially varying cutoff frequency occurs at $f_{co} = 9vm/4\pi\rho$, where v equals the velocity of light in water. For the multiple mode structure, the voltage at any location across the segment is the sum of the mode voltages and can be described as,

$$V(\phi) = A_o + A_2 \cos(9\phi) + A_4 \cos(18\phi) + \ldots \qquad (3)$$

Figure 5 shows the voltage variation of the TEM, m=2 and m=4 modes across the segment. Since the width of the disk segment is a function of the radius of the disk transformer, the cutoff frequency for the TE modes and the transformers efficiency are directly related. As the transformer's electrical length is increased to improve its efficiency, non-TEM losses increase in the disk.

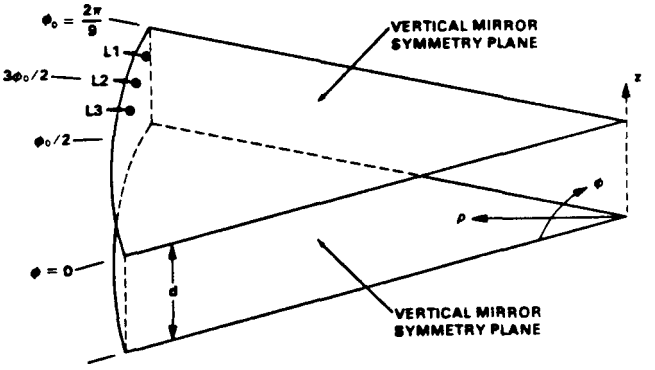

Figure 4. 40 degree disk segment representing a per module equivalent disk transmission line with mirror symmetry planes. Voltage monitor positions are shown by L_1, L_2, and L_3.

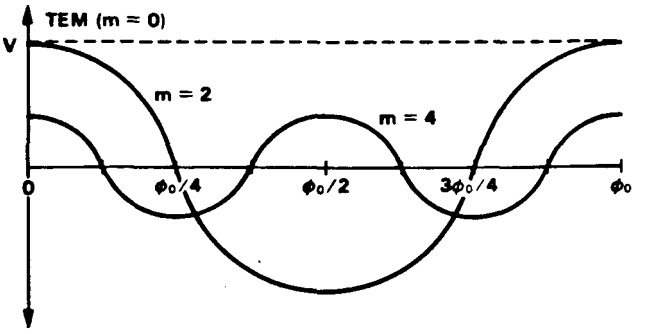

Figure 5. Voltage variation across the disk segment of Fig. 4 for the m=0 (TEM), m=2 and m=4 modes excited by the coax-to-disk transition.

Transition Scale Modeling

Although the mode structure in the disk can be derived, the magnitude of the equivalent energy loss associated with the TE modes is not easily obtained due to the frequency dependent impedances seen by these modes. To quantify the TE mode losses and determine the overall efficiency of the transitions, one-sixth scale, single-module experiments were performed in a configuration that approximates the complex multi-module system of PBFA II. Figure 6 shows the single-module test tank with a lower layer transition installed. The plastic side walls are a good approximation of a magnetic boundary and reproduce the symmetry seen in the multi-module configuration at the inlet to the disk. Tests were performed on a 61 cm wide transition using an injected pulse which represents a one-sixth scale in time PFL output pulse as obtained from the DEMON PFL experiments. Figures 7a and 7b show the scale input pulse and its Fourier transform. The 61 cm transition design has a cutoff frequency for the m=2 TE mode of 55 MHz. Significant energy is available above f_{co} for this transition design as shown in Fig. 7b. With an understanding of the mode structure as indicated in Eq. 3, and appropriate voltage measurements across the transition, extraction of the first three modes is possible. The TEM, m=2 and m=4 modes can be extracted from the monitored voltages by the following relations,

$$V_{TEM} = (V_{L1} + V_{L3})/2 \qquad (4)$$

$$V_{m=2} = 0.5\ (V_{L1} - V_{L3})/0.707 \qquad (5)$$

$$V_{m=4} = -(V_{L2} - V_{TEM}) \qquad (6)$$

V_{L1}, V_{L2} and V_{L3} are voltage monitor waveforms at the locations shown in Fig. 4, which are spaced in increments of $\phi_0/8$ from the segment edge. These waveforms and the extracted mode voltages are shown in Fig. 8.

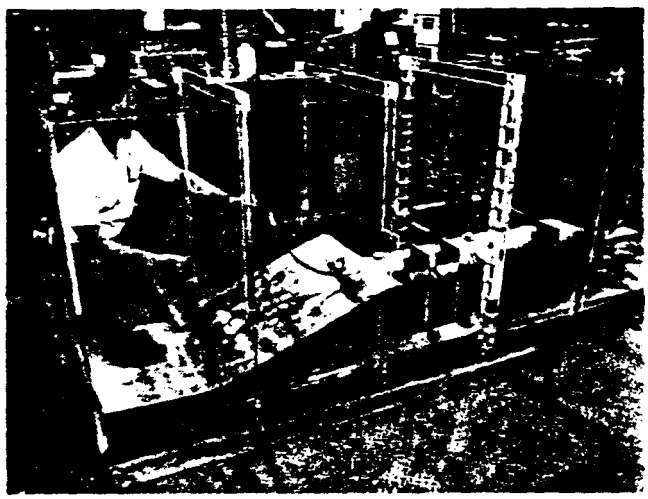

Figure 6. Single-module, one-sixth scale test configuration to determine non-TEM losses in the 61 cm transition.

The TEM waveform at the inlet to the equivalent disk represents the usable forward-going energy delivered by the transition in this specific geometry. Since the radially directed TEM waveform propagates in the known TEM line impedance, its energy content is readily obtained and defines the transitions overall efficiency. This TEM waveform is a crucial input to the full system circuit models used to optimize the upgrade component designs and predict the efficiency of the multi-module system. The single-module test configuration, however, has a different TEM equivalent circuit, at the transition junction, when compared to the multi-module TEM system of Fig. 3. The difference in the TEM equivalent junction circuits must be taken into account in order to predict the efficiency of this transition design in the multi-module configuration. By calculating the TEM circuit for the single module test, the non-TEM losses can be determined for the specific design. Transition losses which exceed the calculated TEM junction losses represent the non-TEM losses. Since these losses depend primarily upon the segment width, they should be very similar in either the single-module or multi-module configuration. This is a key point which allows the single module data to be used as an accurate predictor of the transitions performance in the multi-module system.

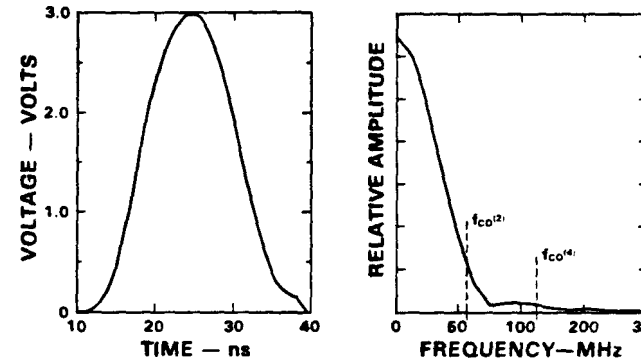

Figure 7. (a) One-sixth scale model input pulse derived from full-scale DEMON experiments of the upgrade PFL system. (b) Fourier Transform of the one-sixth scale pulse.

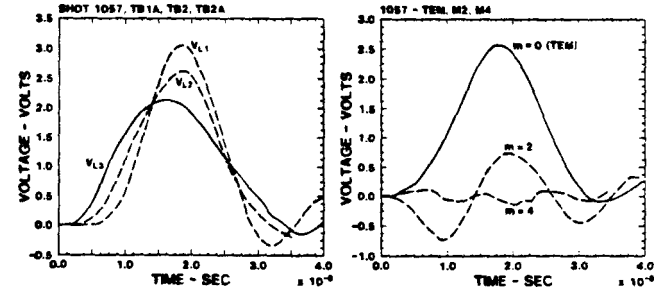

Figure 8. (a) Voltage waveforms V_{L1}, V_{L2} and V_{L3} at the inlet to the disk. (b) Mode voltages as extracted from multi-mode voltage measurements. The m=4 mode contains very little energy in the 61 cm transition.

Once the non-TEM losses were established for a given transition design, the efficiency of the transitions could be established for both layers in the multi-module system. The 61 cm transition yielded projected multi-module efficiencies of 55% and 71% for the upper and lower layers respectively.

Details of initial single module experiments are discussed in Reference 4, which describes the excellent agreement between theory, 3-D, time-dependant EM code analyses and initial transition scale modeling results.

Table 1
Single-Module Scale Model Results and Circuit Model Predictions
61 cm Transition, no blocking cores

Single-Module Scale Experiment				Multi-Module Scale Experiment Predictions					
Transition	Calculated TEM Efficiency	Measured Efficiency	Non-TEM Losses	Calculated TEM Efficiency	Non-TEM Losses	Calculated Transition Efficiency	Calculated Transformer Efficiency	Calculated Stack Coupling Efficiency	Projected Overall System Efficiency
Upper	0.92	0.80	0.13	0.64	0.13	.55	0.8	0.64	0.32
Lower	0.89	0.77	0.13	0.82	0.13	.71			

Full System Design

Once the transitions were characterized, the disk transformer impedance profile was optimized to transport the output pulse to the vacuum stack. A detailed, 2-D, full-system circuit model of two layers of PBFA-II was constructed using the SCREAMER circuit code [6] to predict the performance of the closed disk transformers, flux excluders, and vacuum stack adder. The flux excluder, that is required to properly grade the voltage across the insulator stack, is shown in the lower half of Fig. 1. Concerns that this region of the design may excite higher-order-modes and therefore not be correctly modeled in this full-system circuit model were resolved by the construction of a full detail, 2-D, time-dependent, EM code simulation of the transformer and vacuum stack geometry. Waveform agreement between the EM code and the full-system circuit model were within 2% in energy, which ruled out any significant mode conversion in the closed geometry system.

The input waveforms to each layer in the circuit model were obtained from the measured TEM waveforms at the transition outputs in the single-module experiments. With the transition efficiencies defined, the overall system efficiency, from the PFL's to the vacuum inductance, can be estimated. The efficiency of the transformer design and coupling efficiency from the output of the transformer to the vacuum stack inductance were also determined and are shown in Table 1 with a summary of single-module test data and circuit model predictions.

The efficiency of the overall system is defined as the ratio of the energy stored in the inductance, from the water/plastic interface to the POS location, to the total input energy in a 16.7 ns window (100 ns on a full scale basis).

18-Module Scale Experiment

With the optimization of the transport system complete, a detailed two-layer, 18-module, one-sixth scale model of PBFA II was constructed to address any 3-D effects not modeled at this point in the project. The scale model required stringent mechanical tolerances to allow high confidence measurements, with absolute accuracies of better than 2% in voltage and current. The one-sixth scale model is shown in Fig. 9.

As mentioned earlier, the attainable transition efficiencies are limited by the present physical spacings in the PFL region of PBFA II. The TEM losses in the transition junction can be reduced substantially with the use of magnetic blocking cores to raise the external shunt impedances. This concept was tested with the use of TDK ferrite-type PE11B cores (45cm OD x 25.4cm ID x 2.54 cm width) around both the upper and lower layer coaxes just prior to the transitions. Due to a limited supply of ferrite cores and spacing problems when installing cores on both layers together, cores were tested only on one layer at a time. The ferrite cores were characterized in a separate experiment to determine an impedance model at the high frequencies and low voltages used in the scale model testing. These tests indicated a blocking impedance of approximately 70 ohms. The results from the multi-module TEM circuit analysis of the effect of cores on the top only, bottom only, and both layers are shown in Table 2, which compares the predicted efficiencies with measurement results from the 18-module experiment.

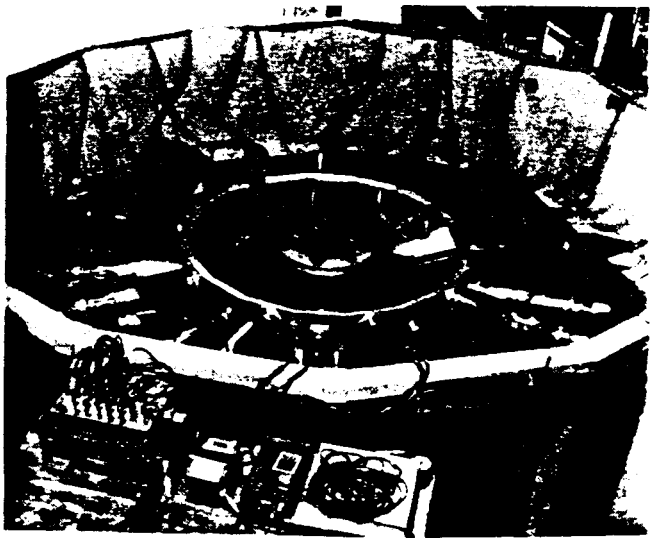

Figure 9. Eighteen module, one-sixth scale experiment with full detail vacuum stack, flux-excluders, transformers and transitions. A region of disk lines have been removed to show the profile of the disk transformers.

Table 2
Comparison of Predicted System Performance
To Results of 18-Module Experiments

18-Module Scale Experiment Predictions				18-Module Scale Model Measurements
Trans.	Calculated TEM Efficiency	Transition Efficiency Including TE Losses	Overall Eff.	Overall Sys. Efficiency
	No Cores			
Upper	.64	.55	.32	.32
Lower	.82	.71		
	Cores on Top Only			
Upper	.87	.76	.38	.36
Lower	.83	.72		
	Cores on Bottom Only			
Upper	.82	.71	.37	.36
Lower	.85	.74		
	Cores on Both Layers			
Upper	.88	.77	.39	Not Measured
Lower	.88	.77		

Based on the 18-module experimental results and the energy measurements from the DEMON upgrade PFL experiments, a comparison to the present PBFA II system can be made. It should be noted that Metglas cores would be used in PBFA II and will perform substantially better than the ferrite cores did in the scale experiments. Based on preliminary circuit modeling, Metglas cores should provide blocking impedances of 500 Ω or greater. For 500 Ω cores on both layers, the calculated TEM efficiency would improve to 95% for the upper and lower layers. The performance of the upgrade system with the the 70 Ω Ferrite cores and 500 Ω Metglas cores are shown in Table 3 for various upgrade options.

Table 3
Summary of Projected Overall System Performance for Various Upgrade Options
Metglas core estimates are shown in parenthesis.

Transmission System	Overall System Efficiency	Energy Stored in Vacuum Inductance MJ	% Gain
Present PBFA II	0.28	2.0 +/- 0.2(1)	0
Upgrade Design			
No Cores	0.32	2.3 +/- 0.1	15 +/- 2
Cores on Top Only	0.38 (0.41)	2.7 +/- 0.1 (2.9 +/- 0.1)	35 +/- 4 (45 +/- 5)
Cores on Both Layers	0.39 (0.43)	2.8 +/- 0.1 (3.1 +/- 0.1)	40 +/- 4 (55 +/- 6)

(1) Based on 3.4 +/- .2 MA per side and 170 nH stack inductance per side.

Summary

Within the constraints of limited hardware changes, an upgrade for PBFA II has been designed and characterized. The upgrade design increases the energy coupled to the inductance of the vacuum stack by more than 50% over the existing system. This gain was accomplished through an analytical approach to understanding the fundamental nature of loss mechanisms in open geometry systems and in components which have physical dimensions which are an appreciable fraction of the source wavelength. The appropriate use of TEM circuit modeling and scale model experiments to analyze a complex 3-D system has yielded excellent agreement and demonstrated the predictive capabilities of such techniques to model and optimize the PBFA II pulsed-power system.

Acknowledgement

The authors wish to thank M. Wilson of Sandia National Laboratories, B. Kirby and D. Rogers of Lawrence Livermore National Laboratories for the timely loan of ferrite cores to complete this research. The authors thank J. Cap, J. Puissant, M. Herman, Z. Ziska, and M. Butler for their diligent help in the scale model experiments.

References

1. E. L. Neau, J. F. Seamen, D. D. Bloomquist, S. R. Babcock, L. X. Schneider, and B. R. Sujka, "A Comparison of Energy Transport Measurements and Computer Simulations in a Single Module Prototype for PBFA II," in Proceedings of the 5th Pulsed-Power Conference, Arlington, VA, June 10-12, 1985, pp. 772-775.
2. P. Sincerny, M. Krishnan, D. Drury, S. Arnold, I. Roth, G. James, and T. Warren, "FALCON and Inductive Store/Opening Switch X-ray Simulator Test Bed", presented at the 7th IEEE Pulsed Power Conference, Monterey, CA, June 11-14, 1989
3. W. A. Johnson, L. X Schneider, E. L. Neau, "TEM Analysis and Computer Simulations of DEMON and PBFA-II Open Transmission Line Systems", in Proceedings of the 6th IEEE Pulsed-Power Conference, Arlington, VA, June 6-7, 1987,
4. W. A. Johnson and L. K. Warne, "TEM Analysis of Multi-Module Effects on Coax-Parallel-Plate Transitions for PBFA II, submitted to Laser and Particle Beams,
5. W. A. Johnson, L. X Schneider, E. L. Neau, "Theory, Simulation, and Experiment of a Single Module Coax-to-Parallel Transition for the Transformer Section of PBFA II", Proceeding of 7th IEEE Pulsed Power Conference, June 11-14, 1989, Monterey, CA.
6. M. L. Kiefer and M. M. Widner, "SCREAMER - A Single-Line Pulsed-Power Design Tool," in Proceedings of the 5th Pulsed-Power Conference, Arlington, VA, June 10-12, 1985, pp. 685-688.